

Unlocking synchrotron sources for THz spectroscopy at sub-MHz resolution: supplement

T. S. HEARNE,^{1,*}  M.-H. MAMMEZ,² D. MAMMEZ,² M.-A. MARTIN-DRUMEL,¹  P. ROY,³ O. PIRALI,^{1,3} S. ELIET,⁴ S. BARBIERI,⁴ F. HINDLE,³ G. MOURET,³  AND J.-F. LAMPIN⁴

¹Université Paris-Saclay, CNRS, Institut des Sciences Moléculaires d'Orsay (ISMO), 91405 Orsay, France

²Laboratoire de Physico-Chimie de l'Atmosphère (LPCA), Université Littoral Côte d'Opale, Avenue Schumann, F-59140 Dunkerque, France

³Synchrotron Soleil, L'Orme des Merisiers Saint Aubin, BP 48, 91192 Gif-sur-Yvette, France

⁴Univ. Lille, CNRS, Centrale Lille, Univ. Polytechnique Hauts-de-France, UMR 8520 - IEMN - Institut d'Electronique de Microélectronique et de Nanotechnologie, F-59000 Lille, France

*thomas.hearne@universite-paris-saclay.fr

This supplement published with Optica Publishing Group on 18 February 2022 by The Authors under the terms of the [Creative Commons Attribution 4.0 License](#) in the format provided by the authors and unedited. Further distribution of this work must maintain attribution to the author(s) and the published article's title, journal citation, and DOI.

Supplement DOI: <https://doi.org/10.6084/m9.figshare.18517937>

Parent Article DOI: <https://doi.org/10.1364/OE.448147>

Unlocking synchrotron sources for THz spectroscopy at sub-MHz resolution: supplemental document

1. Supplementary Methods

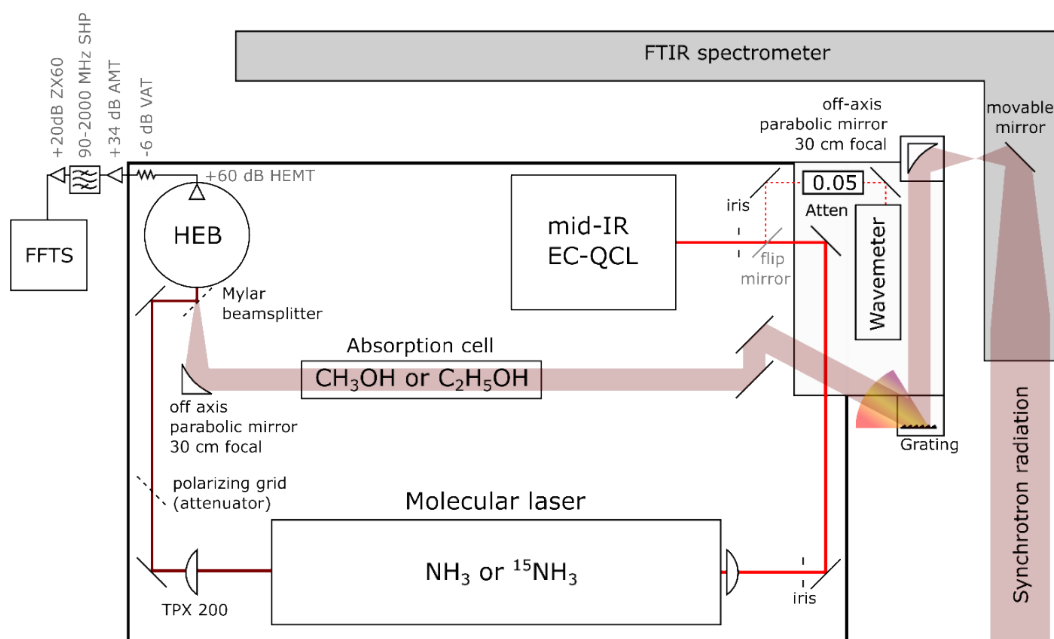


Figure S1. Detailed implementation THz heterodyne spectrometer on the AILES beamline of SOLEIL. The synchrotron radiation (pink) is extracted on the right, where it can be passed either to the THz heterodyne spectrometer (via an off-axis parabolic mirror which collimated the synchrotron source to a beam of diameter 5 cm) or to the Fourier-transform infrared (FTIR) spectrometer by removing the first mirror. In the heterodyne setup, the synchrotron beam diffracts from the grating, which serves as a bandpass filter, before passing through the absorption cell and is then focused by an off-axis parabolic mirror through a mylar beamsplitter onto the HEB. The mid-IR pump laser path (bright red) can be diverted through an attenuator with an attenuation factor of 0.05 to a wavemeter (dashed red line) to verify the pump laser wavelength. The molecular THz laser path (dark red) is attenuated by a polarizing grid to provide the best power for maximising the sensitivity of the hot electron bolometer (HEB) sensitivity. Finally, the block diagram of the IF signal chain, including the HEB pre-amplifier, is shown at the top-left of the graphic.

Post-Processing

The data recorded by the fast Fourier-transform spectrometer (FFTS) underwent a series of post-processing procedures before their use in Fig. 2 and Fig. 3 in the main text. Firstly, the data was corrected with a blank recording, before filters were used to remove unwanted spurious and periodic signals in the resulting spectrum. The filtered spectrum was corrected for its baseline, before an optional smoothing and resampling stage. An example spectrum showing the effects of the post-processing routine is given in Fig. S2.

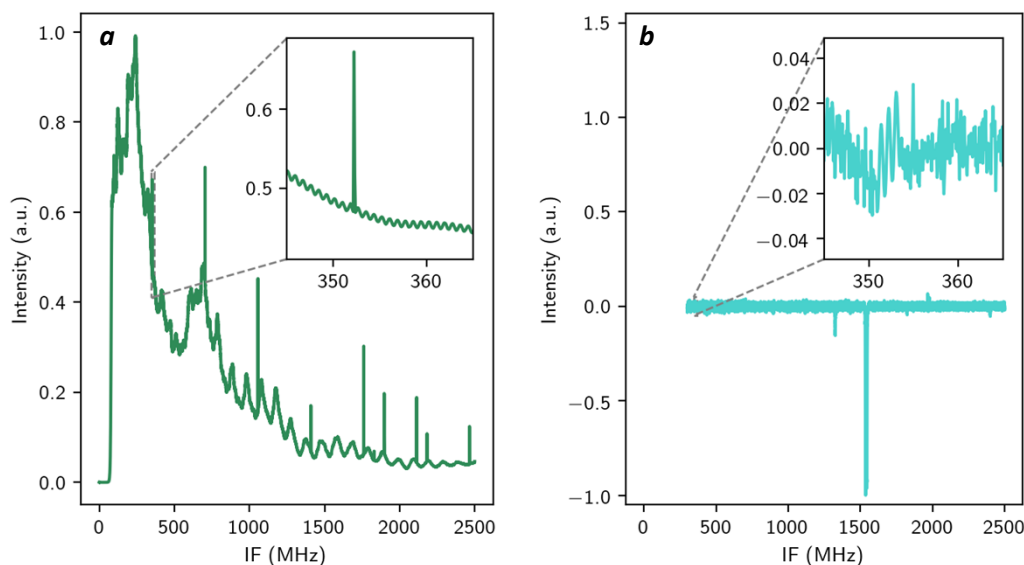


Figure S2. Effects of post-processing. **a**, raw spectrum as recorded by the FFTS without any post-processing. The inset shows a sharp spurious signal at 352 MHz, corresponding to the repetition rate of the synchrotron source, as well as a sinusoidal pattern with 846 kHz spacing. **b**, the final, processed spectrum (see text for details) with spurious signals and regular patterns removed, and a flat baseline. The inset in **b** shows the same region as the inset for **a**, however now only random noise around the baseline is observable.

Blank measurements, with an evacuated absorption cell, were taken before and ideally after each measurement of the absorption of a sample of methanol. The sample spectra were converted into pseudo-transmission spectra by dividing by the blank spectra. However, the values should not be considered as true transmission, since the baseline was observed to vary significantly between recordings. This is thought to be due to short-term fluctuations in the intensity of the molecular laser and synchrotron output and hence the use of the term “pseudo-transmission” in the main text.

The inset in Supplementary Fig. S2(a) shows an example of a sharp spurious line in the recorded spectrum. They have many possible origins; prominent examples are the strong spurious lines spaced by 352 MHz, which is the repetition rate of the synchrotron source. Since spurious content tends to be non-Gaussian in profile, and often only a few points wide, it is possible to reject spurious data points with high discrepancy and minimal loss of spectral data. This was achieved by taking the second derivative of the data. Spurious points were defined as those with a second derivative value more than 2 times above the root-mean-square (RMS) noise value of the second derivative data. Importantly, the second derivative of molecular transition peaks was always below the noise level. The spurious points were then removed and replaced with linear interpolation between averages of the 3 points on either side of the deleted points.

Periodic signals that were present in the recorded frequency-domain spectra, such as an often-observed sinusoidal signal of 846 kHz spacing (present in the inset of Fig. S2(a)), were removed using a Chebyshev II-type infinite impulse response (IIR) bandstop filter. After the filtering stages, the baseline for each scan was calculated using the doubly-reweighted penalized least-squares (DRPLS) baseline fitting algorithm. [1] If interference fringes were recorded in the original data, they could not be completely removed through filtering or baseline fitting without significantly altering the lineshape of the recorded transitions. However, if the baseline of the blank and the active records were well matched before any post-processing, the intensity of the interference fringes was minimised.

The room temperature Doppler full-width at half maximum (FWHM) of a methanol transition at 1 THz is around 2.2 MHz, which is about 28 data points in the FFTS output (at 80 kHz resolution). Since the spectrum is quite heavily oversampled for typical room-temperature methanol line-widths, a Savitzky–Golay filter of the 4th order was used to smooth the data, before it was resampling by a factor of 1/7 (to a resolution of 540 kHz), for Fig. 4 in the main text. The smoothing and resampling also improves the signal-to-noise ratio (SNR) of the recorded peaks.

Data Fitting

Two different fitting approaches were used for the data presented in this work. Fitting of pressure broadening data, and the THz comb mixed with molecular laser beat note positions was preformed using an implementation in the “lmfit” python package of the Levenberg–Marquardt non-linear least-squares algorithm. [2] Lineshape fitting (which often requires comprehensive adjustment of many different variables for a good fit) was performed with the “ampgo” algorithm for finding global minima. [3] Peak fitting was performed on unsmoothed data with as little post-processing as possible in order to preserve the underlying lineshape. Furthermore, peaks comprising of more than two overlapping transitions, or with interference from spurious content, or with low SNR compared to the interference fringes, were excluded from the peak fitting routine. Table S1 contains the complete list of peaks which have been assigned to specific methanol and ethanol transitions fit to a Voigt profile, and included in subsequent analysis in the main text and in the supplementary information.

For the determination of line positions in the IF and Doppler broadening determinations, peaks were fit to a Voigt profile with a floating Gaussian FWHM and a Lorentzian FWHM fixed to an estimated pressure broadening FWHM. Fitting windows were defined close to the visible edge of the peak. However, overlap between the fringes of the peaks and interference fringes distorts the shape of the line at points far from the peak position. Some lines which were partially overlapping were fit simultaneously with the sum of 2 different Voigt profiles. Other lines with very small splitting (<10 kHz) were treated as a single transition, so are assumed to have identical Gaussian and Lorentzian FWHMs and an averaged frequency. Further fitting was performed with a Gaussian width fixed to the expected room temperature Doppler FWHM with a floating Lorentzian FWHM. The obtained Lorentzian widths were then fit linearly against the recorded pressure in order to obtain estimates of the pressure broadening rates of different transitions.

2. Supplementary Results

Table S1. Methanol and Ethanol transition assignments and parameters as determined by fitting a Voigt profile to lines in the THz heterodyne spectra. The given uncertainties are the 95% confidence interval (CI) of the fit. The LO frequency is assumed to be the HITRAN literature value for the ammonia transition targeted in the lasing scheme [4], but the uncertainty in this value is large (up to 2.5 MHz). This uncertainty (and any other sources of uncertainty, such as pressure shifting) is not included in the fit uncertainty. The predicted transition frequencies as given by the JPL database are also shown [5], along with the difference between the literature and experimental values.

Transition	Frequency fit to experiment (MHz)	Fit Uncertainty (MHz)	JPL prediction (MHz)	Difference (MHz)	Gaussian FWHM ^a (MHz)
LO = 1035.2013 GHz – ethanol ^b					
35(11,24) ⁺ - 34(10,24) ⁻ and 35(11,25) ⁺ - 34(10,25) ⁻	1033387.067 ^c	0.036	1033384.641	2.426	2.41(51)
38(10,28) ⁺ - 37(9,28) ⁻	1034063.219	0.120	1034060.793	2.426	1.03(50)
34(9,26) - 33(8,25)	1034185.298	0.032	1034182.645	2.653	1.89(26)
32(8,24) ⁻ - 31(7,24) ⁺	1035138.324	0.112	1035135.951	2.373	1.24(36)
16(15, 1) - 15(14, 1) and 16(15, 2) - 15(14, 2)	1035333.121 ^c	0.006	1035330.488	2.633	1.96(5)
32(8,25) ⁻ - 31(7,25) ⁺	1035400.022	0.026	1035397.162	2.860	2.64(25)
19(14, 5) - 18(13, 6) and 19(14, 6) - 18(13, 5)	1036062.873 ^c	0.009	1036060.256	2.617	1.95(7)
31(10,22) - 30(9,21)	1036176.159	0.027	1036173.698	2.461	1.35(12)
31(10,21) - 30(9,22)	1036190.662	0.025	1036188.203	2.459	2.10(19)
28(11,18) - 27(10,17)	1036599.198 ^c	0.021	1036596.670	2.528	1.87(17)
22(13, 9) - 21(12,10) and 22(13, 10) - 21(12,9)	1036667.492 ^c	0.007	1036664.926	2.566	1.81(6)
25(12,13) - 24(11,14)	1037050.898 ^c	0.011	1037048.364	2.534	1.83(8)
LO = 1044.4973 GHz – methanol ^d					
6(-5) - 5(-4) $v_t=0$	1042523.850	0.016	1042521.713	2.137	2.19(20)
8(7) - 9(6) $v_t=0$	1044271.835	0.152	1044269.390	2.445	3.43(167)
21(2) - 20(1) $v_t=0$	1045875.633	0.076	1045873.093	2.540	2.26(22)
LO = 1073.0499 GHz – methanol ^d					
9(4) ⁻ - 8(3) ⁻ $v_t=0$	1071504.798	0.012	1071505.271	-0.473	2.58(3)
9(4) ⁺ - 8(3) ⁺ $v_t=0$	1071513.495	0.010	1071513.929	-0.434	2.60(2)
19(3) ⁺ - 20(2) ⁺ $v_t=1$	1071724.321	0.050	1071724.934	-0.613	2.41(13)
27(2) ⁺ - 26(3) ⁺ $v_t=0$	1072798.877	0.018	1072799.338	-0.461	2.23(6)

LO = 2029.2012 GHz – methanol ^d					
13(9) ⁺ - 13(8) ⁻ $v_t=0$	2026773.300	0.024	2026774.027	-0.727	4.65(5)
12(9) ⁺ - 12(8) ⁻ $v_t=0$	2026846.427 ^e	0.032	2026847.067	-0.640	4.53(4)
11(9) ⁺ - 11(8) ⁻ $v_t=0$	2026908.084	0.054	2026909.336	-1.252	4.50(3)
10(9) ⁺ - 10(8) ⁻ $v_t=0$	2026961.254	0.040	2026962.098	-0.844	4.40(7)
9(9) ⁺ - 9(8) ⁻ $v_t=0$	2027005.445	0.046	2027006.491	-1.046	4.37(10)
28(5) ⁺ - 28(8) ⁺ $v_t=1$ - $v_t=0$ and 28(5) ⁻ - 28(8) ⁻ $v_t=1$ - $v_t=0$	2027611.813 ^e	0.104	2027612.479	-0.699	4.29(17)
5(-4) - 6(-5) $v_t=2$	2027908.304	0.044	2027908.047	0.257	4.27(8)
14(-6) - 13(-5) $v_t=0$	2029484.532	0.012	2029484.648	-0.116	5.08(2)
6(3) ⁻ - 6(2) ⁺ $v_t=1$	2030293.793 ^e	0.054	2030294.113	0.320	4.48(2)
7(3) ⁺ - 7(2) ⁻ $v_t=1$	2030300.104 ^e	0.042	2030301.025	0.166	4.48(2)
7(3) ⁻ - 7(2) ⁺ $v_t=1$	2030323.572	0.022	2030323.596	-0.024	4.51(4)
8(3) ⁺ - 8(2) ⁻ $v_t=1$	2030334.875	0.016	2030335.264	-0.389	4.62(3)
8(3) ⁻ - 8(2) ⁺ $v_t=1$	2030372.815	0.024	2030372.902	-0.087	4.69(3)
9(3) ⁺ - 9(2) ⁻ $v_t=1$	2030388.732	0.262	2030389.084	-0.352	4.64(3)
9(3) ⁻ - 9(2) ⁺ $v_t=1$	2030448.153	0.018	2030448.262	-0.109	4.85(3)
10(3) ⁺ - 10(2) ⁻ $v_t=1$	2030467.824	0.018	2030467.853	-0.029	4.80(4)
10(3) ⁻ - 10(2) ⁺ $v_t=1$	2030556.302	0.032	2030556.677	-0.375	4.75(4)
11(3) ⁺ - 11(2) ⁻ $v_t=1$	2030577.518	0.026	2030577.522	-0.004	4.56(3)
18(6) ⁻ - 17(5) ⁻ $v_t=0$ and 18(6) ⁺ - 17(5) ⁺ $v_t=0$	2030590.624 ^e	0.028	2030590.780	-0.199	5.04(5)
22(6) ⁻ - 21(5) ⁻ $v_t=1$ and 22(6) ⁺ - 21(5) ⁺ $v_t=1$	2030636.063 ^e	0.030	2030636.431	-0.339	4.66(5)
11(3) ⁻ - 11(2) ⁺ $v_t=1$	2030705.539	0.022	2030705.911	-0.372	4.50(19)
12(3) ⁺ - 12(2) ⁻ $v_t=1$	2030724.575	0.024	2030724.612	-0.037	4.59(20)
12(3) ⁻ - 12(2) ⁺ $v_t=1$	2030904.150 ^e	0.026	2030904.488	-0.338	4.56(7)
13(3) ⁺ - 13(2) ⁻ $v_t=1$	2030916.151 ^e	0.024	2030916.208	-0.067	4.73(5)
14(3) ⁺ - 14(2) ⁻ $v_t=1$	2031160.062 ^e	0.104	2031159.950	0.112	4.65(12)
15(3) ⁺ - 15(2) ⁻ $v_t=1$	2031463.944	0.032	2031464.023	-0.079	4.39(6)
LO = 2064.9399 GHz – methanol ^d					

12(-7) - 11(-6) $v_t=0$	2064091.427	0.058	2064091.940	-0.513	4.76(13)
18(5) ⁺ - 17(4) ⁺ $v_t=0$	2066892.128	0.134	2066892.1	0.028	3.73(25)
18(5) ⁻ - 17(4) ⁻ $v_t=0$	2066913.214	0.162	2066913.102	0.112	4.74(38)
11(9) - 10(8) $v_t=0$	2067176.536	0.200	2067176.557	-0.021	4.99(43)
LO = 2822.2564 GHz – methanol ^d					
15(-12) - 14(-11) $v_t=0$	2823435.737	0.068	2823435.303	0.434	5.86(10)
LO = 3373.6130 GHz – methanol ^d					
14(7) ⁺ - 14(6) ⁻ $v_t=1$	3371174.497	0.214	3371176.007	-1.510	7.20(63)
20(6) - 20(5) $v_t=1$	3372020.599	0.294	3372020.985	-0.386	7.45(80)
15(7) ⁻ - 15(6) ⁺ $v_t=1$ and 15(7) ⁺ - 15(6) ⁻ $v_t=1$	3372337.191 ^c	0.064	3372337.645	-0.458	8.09(21)
37(8) ⁺ - 36(7) ⁺ $v_t=0$ and 37(8) ⁻ - 36(7) ⁻ $v_t=0$	3372568.239 ^c	0.488	3372569.991	-1.868	6.17(22)
2(2) - 3(3) $v_t=2$ - $v_t=1$	3372759.229	0.068	3372759.952	-0.723	7.63(18)
8(0) ⁺ - 9(1) ⁻ $v_t=2$ - $v_t=1$	3373886.486	0.114	3373888.999	-2.513	8.59(45)
17(7) ⁻ - 17(6) ⁺ $v_t=1$ and 17(7) ⁺ - 17(6) ⁻ $v_t=1$	3375499.942 ^c	0.088	3375501.051	-1.109	7.17(107)

^a Gaussian width determined using a Voigt profile with a Lorentzian FWHM fixed to a value estimated using the HITRAN self-pressure broadening rate (12 MHz mbar⁻¹) and the recorded pressure.

^b Ethanol transitions labelled with rotational constants in the format $J(K_a, K_c)$ and a superscript symbol for the parity of the gauche conformer, the trans conformer indicated by an absence of a superscript symbol.

^c Transition fit as an average of two closely spaced lines.

^d Methanol transitions labelled with rotational constants in the format $J(K)$ with a superscript parity symbol for A-state transitions. E-state transitions have no superscript symbol, with an unsigned (positive) K denoting the E1-state, and a negative sign on K denoting the E2-state. The torsional mode v_t , and its change, if applicable, is also given.

^e Transition fit using the sum of two Voigt profiles.

Pressure Broadening Analysis

A rudimentary analysis of self-pressure broadening of methanol was carried out with methanol using the THz heterodyne spectrometer. Between two and four different pressures of methanol were used in total in these experiments, allowing a limited estimation of the self-pressure broadening rate for most transitions listed in Table S1. The weighted average of the calculated rates comes to 14.4 MHz mbar⁻¹, which is not far from the HITRAN assumed value of 12 MHz mbar⁻¹. [4] Despite the small quantity of available data, most of the pressure broadening rates fall within a reasonable range from 8 to 20 MHz mbar⁻¹. For comparison, Slocum *et al.* found a range of 5 to 20 MHz mbar⁻¹ for self-broadening of methanol transitions between 1.480-1.495 THz. [6] The pressure of methanol used to produce the data shown here was around 50 μ bar, which gives a pressure-broadening FWHM of 0.6 MHz. According to the data of Slocum *et al.*, this value could be as high as 1 MHz, or as low as 0.25 MHz. The use of an incorrect pressure broadening FWHM could negatively influence the Gaussian FWHM determined in Table S1,

however, the good agreement between the determined Gaussian FWHMs and the expected Doppler FWHMs (shown in Fig. 3 in the main text) implies that this variation from the HITRAN value has minimal impact for most of the transitions observed in these experiments.

References

1. J. Ye, Z. Tian, H. Wei, and Y. Li, "Baseline correction method based on improved asymmetrically reweighted penalized least squares for the Raman spectrum," *Appl. Opt.* **59**, 10933–10943 (2020).
2. Matt Newville, Renee Otten, Andrew Nelson, Antonino Ingargiola, Till Stensitzki, Dan Allan, Austin Fox, Faustin Carter, Michał, Dima Pustakhod, Yoav Ram, Glenn, Christoph Deil, Stuermer, Alexandre Beelen, Oliver Frost, Nicholas Zobrist, Gustavo Pasquevich, Allan L. R. Hansen, Tim Spillane, Shane Caldwell, Anthony Polloreno, andrewhannum, Julius Zimmermann, Jose Borreguero, Jonathan Fraine, deep-42-thought, Benjamin F. Maier, Ben Gamari, and Anthony Almaraz, *Lmfit/Lmfit-Py 1.0.0* (Zenodo, 2019).
3. L. Lasdon, A. Duarte, F. Glover, M. Laguna, and R. Martí, "Adaptive memory programming for constrained global optimization," *Comput. Oper. Res.* **37**, 1500–1509 (2010).
4. I. E. Gordon, L. S. Rothman, C. Hill, R. V. Kochanov, Y. Tan, P. F. Bernath, M. Birk, V. Boudon, A. Campargue, K. V. Chance, B. J. Drouin, J.-M. Flaud, R. R. Gamache, J. T. Hodges, D. Jacquemart, V. I. Perevalov, A. Perrin, K. P. Shine, M.-A. H. Smith, J. Tennyson, G. C. Toon, H. Tran, V. G. Tyuterev, A. Barbe, A. G. Császár, V. M. Devi, T. Furtenbacher, J. J. Harrison, J.-M. Hartmann, A. Jolly, T. J. Johnson, T. Karman, I. Kleiner, A. A. Kyuberis, J. Loos, O. M. Lyulin, S. T. Massie, S. N. Mikhailenko, N. Moazzen-Ahmadi, H. S. P. Müller, O. V. Naumenko, A. V. Nikitin, O. L. Polyansky, M. Rey, M. Rotger, S. W. Sharpe, K. Sung, E. Starikova, S. A. Tashkun, J. V. Auwera, G. Wagner, J. Wilzewski, P. Weislo, S. Yu, and E. J. Zak, "The HITRAN2016 molecular spectroscopic database," *J. Quant. Spectrosc. Radiat. Transf.* **203**, 3–69 (2017).
5. H. M. Pickett, R. L. Poynter, E. A. Cohen, M. L. Delitsky, J. C. Pearson, and H. S. P. Müller, "Submillimeter, millimeter, and microwave spectral line catalog," *J. Quant. Spectrosc. Radiat. Transf.* **60**, 883–890 (1998).
6. D. M. Slocum, L.-H. Xu, R. H. Giles, and T. M. Goyette, "Retrieval of methanol absorption parameters at terahertz frequencies using multispectral fitting," *J. Mol. Spectrosc.* **318**, 12–25 (2015).